Preprint
UCRL-JC-146317

X-ray Spectropolarimetry Studies at the Nevada Terawatt Facility and LLNL EBIT

A. S. Shlyaptseva, V. L. Kantsyrev, B. S. Bauer, P. Neill, C. Harris, D. A. Fedin, S. Hansen, N. Ouart, P. Beiersdorfer, A. G. Petrashen, U. I. Safronova

This article was submitted to
The Proceedings of the Third US-Japan Plasma Polarization Spectroscopy Workshop, Livermore, CA, June 18-21, 2001

October 20, 2001

X-ray spectropolarimetry studies at the Nevada Terawatt Facility and LLNL EBIT

A.S. Shlyaptseva, V.L. Kantsyrev, B.S. Bauer, P. Neill, C.Harris, D.A. Fedin, S. Hansen, N. Ouart
(University of Nevada, Reno, USA)

P. Beiersdorfer
(*LLNL, USA*)

A.G. Petrashen
(*IFMO, Russia*)

U. I. Safronova
(*University of Notre Dame, USA*)

Abstract

Recent results from x-pinches at the NTF provide experimental evidence for the existence of strong electron beams in x-pinch plasmas and motivate the development of a new diagnostic, x-ray spectropolarimetry, for investigating the anisotropy of such plasmas. This diagnostic is based on theoretical modeling of polarization-dependent spectra measured simultaneously by spectrometers with different sensitivity to polarization. Results of the first polarization-sensitive experiments at the NTF are presented. K-shell emission from Ti x-pinches is recorded simultaneously by two identical spectrometers with the dispersion plane perpendicular and parallel to the discharge axis. The spectroscopic analysis of more than eight Ti x-pinch shots show how spectropolarimetry complements the usual diagnostics of a z-pinch plasma. The polarization-sensitive spectra, generated by a Maxwellian electron beam at LLNL EBIT have been collected and analyzed. These data make an important contribution to the plasma polarization spectroscopy program at the NTF. In particular, the study of multiply-charged Ti ion spectra help in the interpretation of the polarization-sensitive spectra from Ti x-pinches at the NTF.

I. K-shell x-ray spectropolarimetry of Ti x-pinch plasma at the NTF.

The first polarization-sensitive experiments at the Nevada Terawatt Facility (NTF) have been preformed and prove that the best object for the x-ray spectropolarimetry of high-density plasma is x-pinch plasma. The core of the NTF is a Zebra z-pinch with a maximum voltage 2 MV, a current 1.2 MA, a rise time 100 ns, and a maximum Marx generator energy of 200 kJ (formerly the HDZP-II z-pinch facility at LANL). A x-pinch produces a bright, small-sized x-ray source, with a well-defined location. It can yield x-ray spectra of numerous ions with very high resolution. X-pinches are made by positioning two thin, straight, crossed wires between the cathode and anode of the Zebra pulsed-power generator, with a wire contact at the axis of the cathode-anode gap. Two typical configurations of x-pinches were tested: a wire twisted (at angle of rotation α 30^{o}) and a planar-loop. The most compact, bright source of x-rays was produced using a planar-loop configuration. A schematic view of a x-pinch load with a planar-loop configuration is presented in Fig. 1.

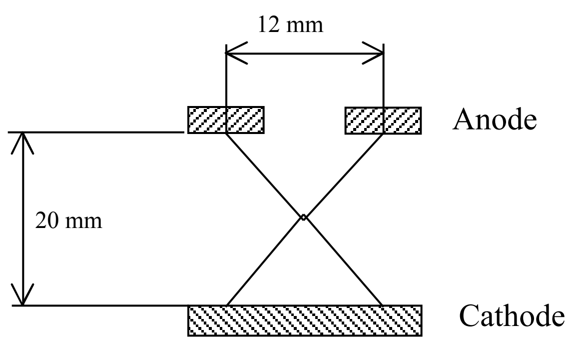

Fig. 1. Planar-loop x-pinch load.

The distinct feature of x-pinches is the existence of a strong electron beam making them attractive objects for spectropolarimetry. A new diagnostic, x-ray spectropolarimetry, applied to x-pinch plasmas, can provide detailed information about the electron distribution function and the magnetic field. Our recent results on x-pinches and x-ray spectropolarimetry have been published [1,2]. Details of K-shell spectroscopy and spectropolarimetry of Ti ions are given below.

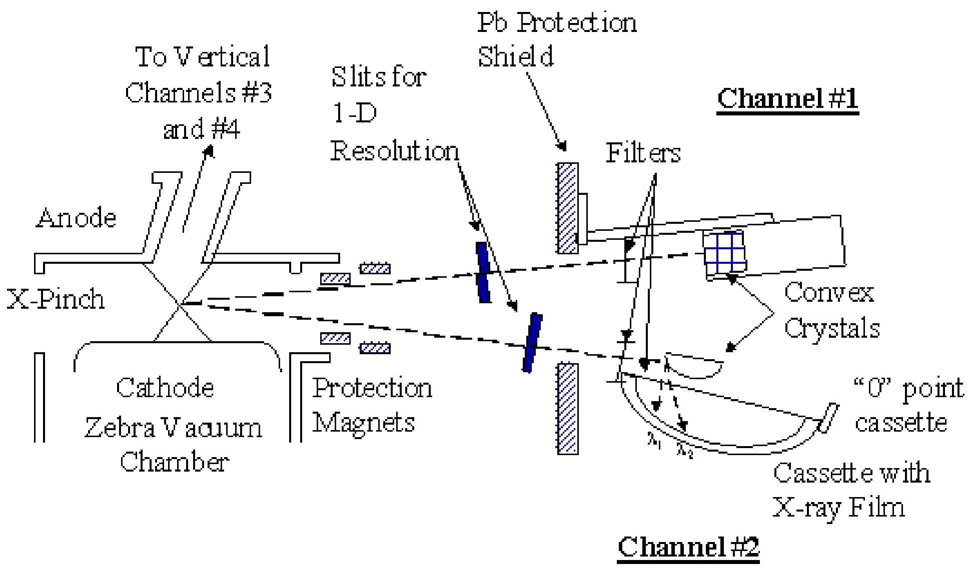

Fig.2. Experimental setup for polarization measurements.

Polarization-sensitive experiments on x-pinch plasmas were performed at the NTF in May-August 2000. The polarization-dependent spectra of Kα line radiation produced by Ti and Fe x-pinches in more than 15 shots were recorded simultaneously by horizontal (with a slit) and vertical (w/o a slit) spectrometers (see experimental setup by Kantsyrev et al [2], Fig. 2). The horizontal spectrometer with a slit provides a resolution along the z-pinch symmetry axis and has a dispersion plane perpendicular to the discharge axis (channel 1), whereas the vertical spectrometer has a dispersion plane parallel to the discharge axis (channel 2). Both spectrometers are identical LiF (2d=4.027 Å) convex crystal spectrometers. The LiF crystal has a spacing corresponding to the nominal Bragg angle of 40º at the wavelength of 2.6 Å: the Ti lines most likely to be polarized with λ close to or above 2.6 Å when a strong electron beam is generated.

Time-integrated images of eight selected shots are shown in Fig.3. In these shots, a planar-loop Ti x-pinch was used as the load (see Fig. 1). The anode is at the top of all images. The brightest spot is located in the cross point of the wires. The cathode is not seen at the bottom.

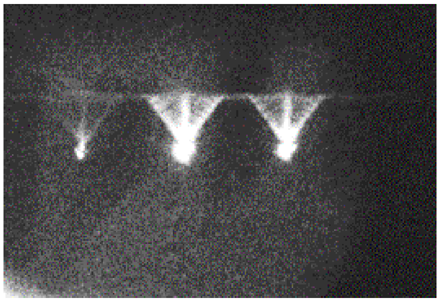

Shot 36 (07/12/00)

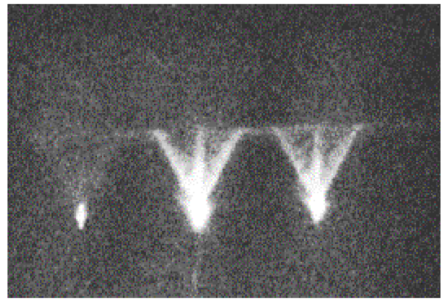

Shot 37 (07/13/00)

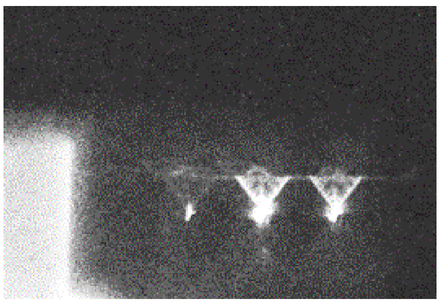

Shot 38 (07/18/00)

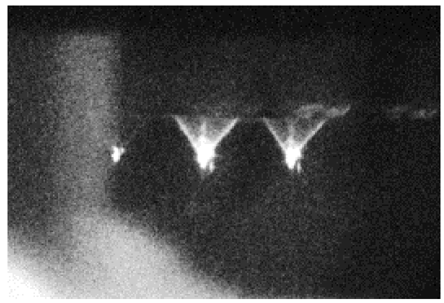

Shot 39 (07/19/00)

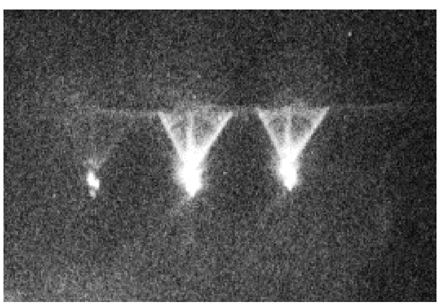

Shot 40 (07/21/00)

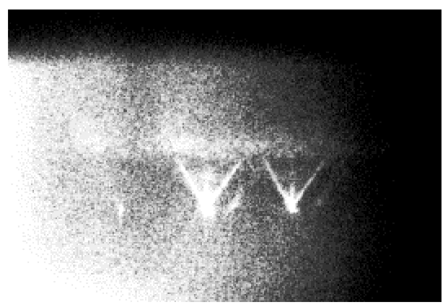

Shot 41 (07/26/00)

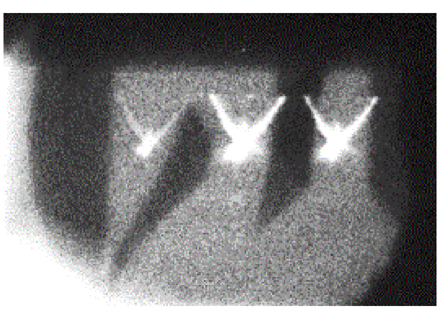

Shot 47 (08/16/00)

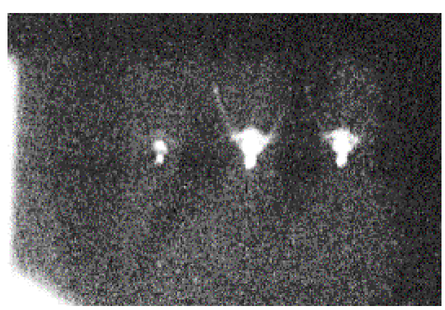

Shot 48 (08/17/00)

Fig. 3. NTF time-integrated x-ray pinhole camera images of Ti x-pinches (shots 36-41, 47 and 48).

The diameter of Ti wires was 30 μ (for the shots 36-41), 76.2 μ (for the shot 47), and 152.4 μ (for the shot 48). The left image in each picture was recorded through the filter providing the maximum of radiation with $\lambda_{1/10} < 2.6$ Å, whereas the center and the right side images were recorded through the filter providing the maximum of radiation with $\lambda_{1/10}$ <7.9 Å and $\lambda_{1/10}$ <5 Å, respectively. Fig. 3 shows that a x-pinch is a small, almost point source of radiation with $\lambda \leq 2.6$ Å, which was also supported by 1-D spectral line measurements. The structure of a x-pinch includes energetic electron beams directed toward the anode and along the wires [1,2]. The experimental estimation of the widths of the central jet on x-pinch x-ray images and Fe K_α spectral lines (generated on a steel anode) has shown that the electron beam diameter in a high-current x-pinch may be smaller than 1mm [3, 4]. As a percentage of the x-pinch discharge energy (E≈100-120 kJ) the electron beam energy is from 2-3 % (for Ti, Fe) to 15-20 % (Mo and W). This is based on the experimental estimation of the energy needed to generate the observed holes at the points of connection of the wires with the anode of a x-pinch [3,4].

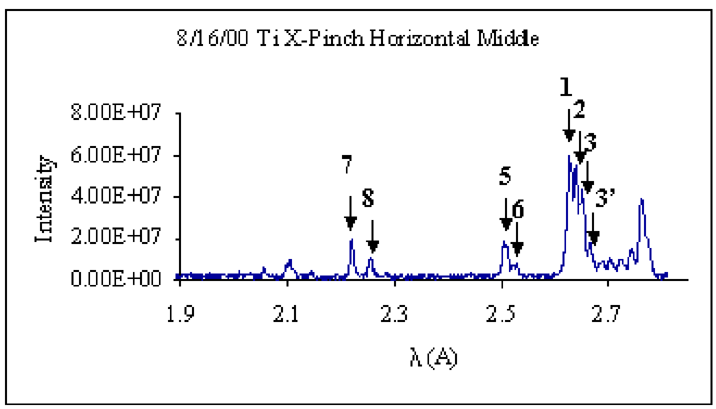

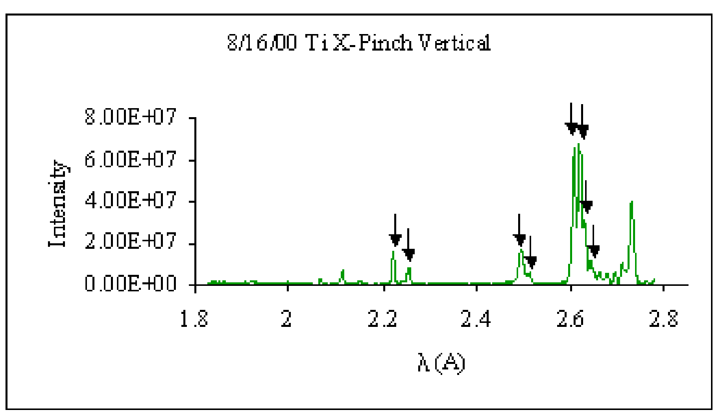

Fig. 4. Polarization-sensitive Ti x-pinch spectra (shot 47).

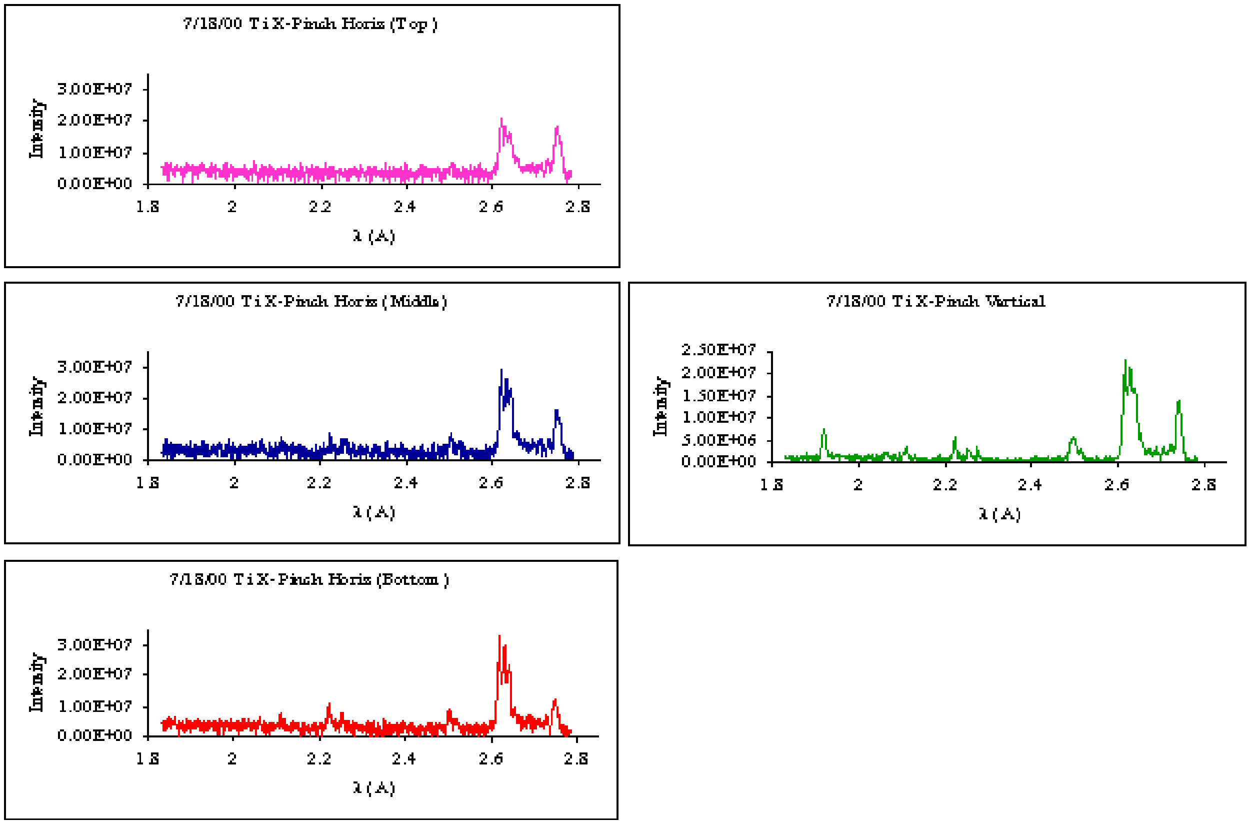

Fig. 5. Polarization-sensitive Ti x-pinch spectra (shot 38).

Typical polarization-sensitive spectra are presented in Figs. 4-5. They include the He-like resonance line Heα (1), the most intense line in all K-shell Ti spectra, the intercombination He-like line y (2), the Li-like satellite line peak (3), the Be-like satellite line peak (3’), the H-like resonance line Lyα (5), the He-like satellite peak (6), the He-like resonance line Heβ (7), and the Li-like satellite peak (8). Also, to the right of the peak 3’, the x-ray spectra include satellite structures due to B-, C-, N-, and O-like Ti ions and the most prominent peak at the right, a cold Kα. Three spatially-resolved spectra recorded by a horizontal spectrometer are presented together with a spectrum recorded by a vertical spectrometer on July 18, 00 (Fig. 5). For the polarization analysis, the horizontal spectra from the middle were chosen. The horizontal spectrometer records mostly parallel polarization state whereas the vertical one records mostly perpendicular polarization state.

Fig. 6 explains the general trends in the polarization of the major lines: the measured ratio of the intensities associated with different polarization states I_{II}/I greater (less) than 1 indicates the positive (negative) polarization of the line. Theoretical calculations estimate that the polarization of the resonance line Heα decreases from 60% at threshold to 0 (near 7 thresholds). It then becomes negative. Polarization of the intercombination line y increases from about –33% (at threshold) to 0 and at higher energies tends to the polarization of the Heα line.

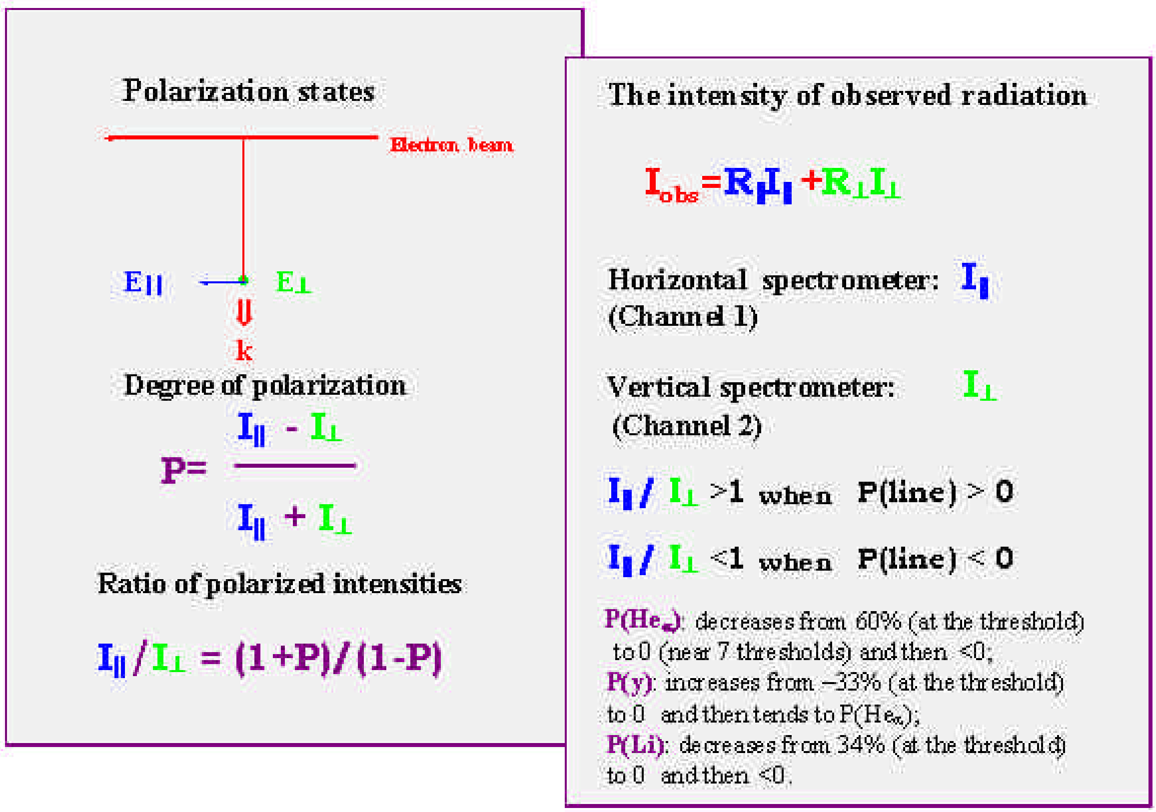

Fig. 6. Identification of the ratio of the intensities of different polarization states ($I_{II}/I_{\perp}$).

Table 1. Illustration of polarization of Ti K-shell lines through the measured ratio of intensities ($I_{II}/I_{\perp}$)

Line		Ion	λ(Å)	7/12/00	7/18/00	7/19/00	7/21/00
1	Heα	He	2.618	0.93	1.02	0.65	1.09
2	y	He	2.631	1.01	0.98	0.66	1.04
3	q	Li	2.640	1.05	1.12	0.86	1.06
3′	sat	Be	2.655	1.0	1.22	1.07	1.13
5	Lyα	H	2.500	0.97	1.25	1.06	1.02
6	sat	H	2.515	1.29	1.58	1.52	1.14
7	Heβ	He	2.221	0.91	1.29	0.69	1.12
8	sat	He	2.253	1.28	1.75	0.94	1.19

The ratios of intensities associated with different polarization states I_{II}/I for each of the spectral lines (1, 2, 3, 3’, 5, 6, 7, and 8), and the line ratios of the intercombination line and satellite lines to their resonance lines (2/1, 3/1, 3’/1, 6/5, and 8/7), from horizontal and vertical are presented in Tables 1,2. Specifically, Table 1 lists the measured ratio of the spectral line intensities associated with different polarization states I_{II}/I for four different shots. The ratios show largest deviation from 1 for the shot on 07/19/00. The ratio for the He-like lines is usually less than 1 (negative polarization), whereas the ratio for most of the satellite peaks is larger than 1 (positive polarization). For example, the data for the shot on 7/19/00 show that the ratio I_{II}/I is 0.65 for the Heα resonance line, 0.66 for the He-like intercombination line y, 0.69 for the Heβ resonance line, whereas this ratio for the satellite peaks is 1.07 for the peak 3’ and 1.52 for the peak 6.

Table 2. Illustration of polarization of Ti K-shell lines through the measured ratio of relative intensities of the lines recorded by a horizontal (H) and vertical (V) spectrometers.

Line ratio	7/12/00 H	V	H/V	7/18/00 H	V	H/V	7/19/00 H	V	H/V	7/21/00 H	V	H/V
2/1	0.90	0.83	1.09	0.88	0.91	0.96	0.88	0.88	1.0	0.82	0.86	0.95
3/1	0.77	0.68	1.13	0.79	0.73	1.1	0.79	0.60	1.32	0.62	0.64	0.98
3'/1	0.30	0.27	1.08	0.33	0.28	1.2	0.33	0.20	1.65	0.35	0.33	1.04
6/5	0.56	0.35	1.61	0.68	0.53	1.27	0.66	0.46	1.42	0.80	0.71	1.13
8/7	0.70	0.50	1.41	0.79	0.58	1.37	0.77	0.57	1.35	0.80	0.75	1.06

Table 2 lists the line ratios of the intercombination line and satellite lines to their resonance lines for the same four shots. The first column for the each shot shows the relative intensities in a spectrum recorded by the horizontal spectrometer, whereas the second column shows the relative intensities in a spectrum recorded by the vertical spectrometer. Both spectra were recorded simultaneously. The third column represents the first column ratio divided by the second column ratio. The data for the 2/1 ratio from the third column indicate almost the same polarization for the Heα and y lines. The ratio for the satellite line peaks to the corresponding resonance lines (3'/1, 6/5, and 8/7) from the third column is larger than 1 for all shots. Summarizing, the data in Tables 1,2 indicate the positive polarization of dielectronic satellite peaks produced by the low energy electron beam (3-5keV) and the negative polarization of resonance lines produced by an electron beam with a much higher energy (>30keV).

X-ray spectral lines of Be-, B-, C-, N-, and O-like Ti ions in the spectral region above 2.6 Å are probably also polarized; relative intensities of corresponding peaks are different in horizontal and vertical spectra.

A collisional-radiative atomic kinetic model has been developed to diagnose the electron temperature and electron beam characteristics of various emitting regions of Ti plasmas produced at the NTF. A detailed description of the model is given in the another publication of this volume (see Shlyaptseva et al , ibid). The NTF Ti spectra exhibit features from H-like Ti to Ti K_α and it is clear that no single region can describe all these features, even with hot electrons. The NTF Ti plasmas are taken to have three regions: a hot, dense region with hot electrons that contributes all of the H-like and most of the He-like radiation, a cooler, less dense region with hot electrons that contributes He- to C-like radiation, and a cool region without hot electron that contributes N- and O-like radiation (the Ti K_α line is not modeled). Three intense T_e-sensitive spectral features useful as temperature diagnostics for the high temperature plasma region are labeled and their dependence on T_e and on hot electrons is shown in Fig. 7. The intensity ratios of Li-like satellite lines to He_α and He_β decrease with increasing T_e, while the intensity of H-like Ly_α increases. The effects of hot electrons are similar to the effects of increasing Te. But if T_e and the hot electron fraction f are chosen such that the increase in the Ly_α intensity is the same in both cases, the Li-like satellites will be more intense with hot electrons than with higher T_e. By matching both the Ly_α and the Li-like satellites to the experimental He_β line, both T_e and f of the hot region can be estimated. The temperature and hot electron dependence of synthetic spectra in the cool region shown in Fig. 8 have a great deal to do with the ionization balance. The regions of emission from the various ionization stages He to O are indicated. At low temperatures, O-like emission dominates. As T_e increases, so does the ionization balance, and the emission is shifted to higher energies. Increasing f has an effect similar to increasing T_e, but, as in the higher temperature case, emission from lower ionization stages is retained. It should be noted that even a very small fraction (10^{-4}) of hot electrons has a significant effect on the ionization balance at low T_e. This is not the case for the high T_e regions, where significant changes require a few percent of hot electrons. The development of x-ray spectropolarimetry can complement kinetic modeling with inclusion of hot electrons by providing an important information on electron beam characteristics.

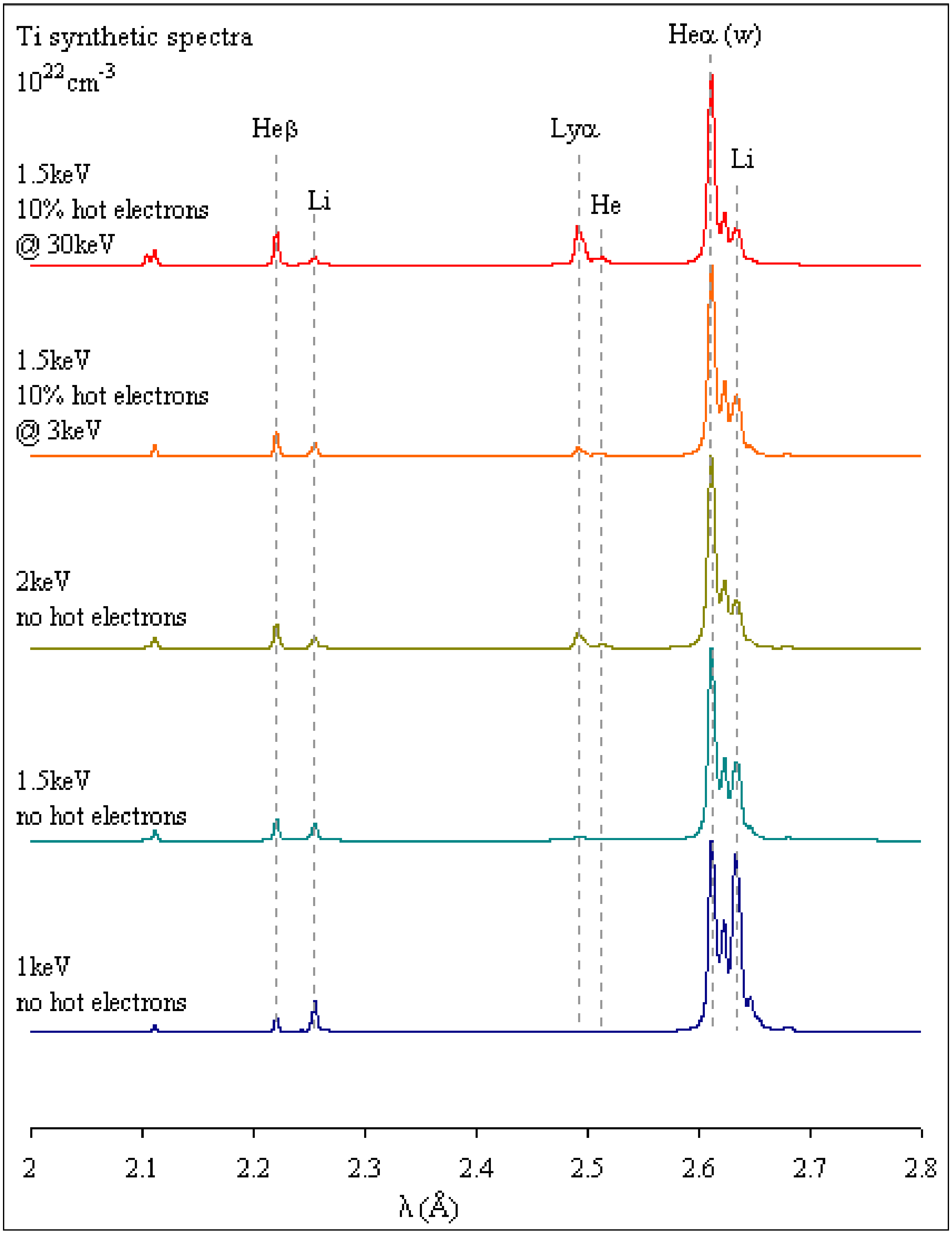

Fig. 7. Effect of Te and hot electrons on the "hot spectral region" of Ti spectra.

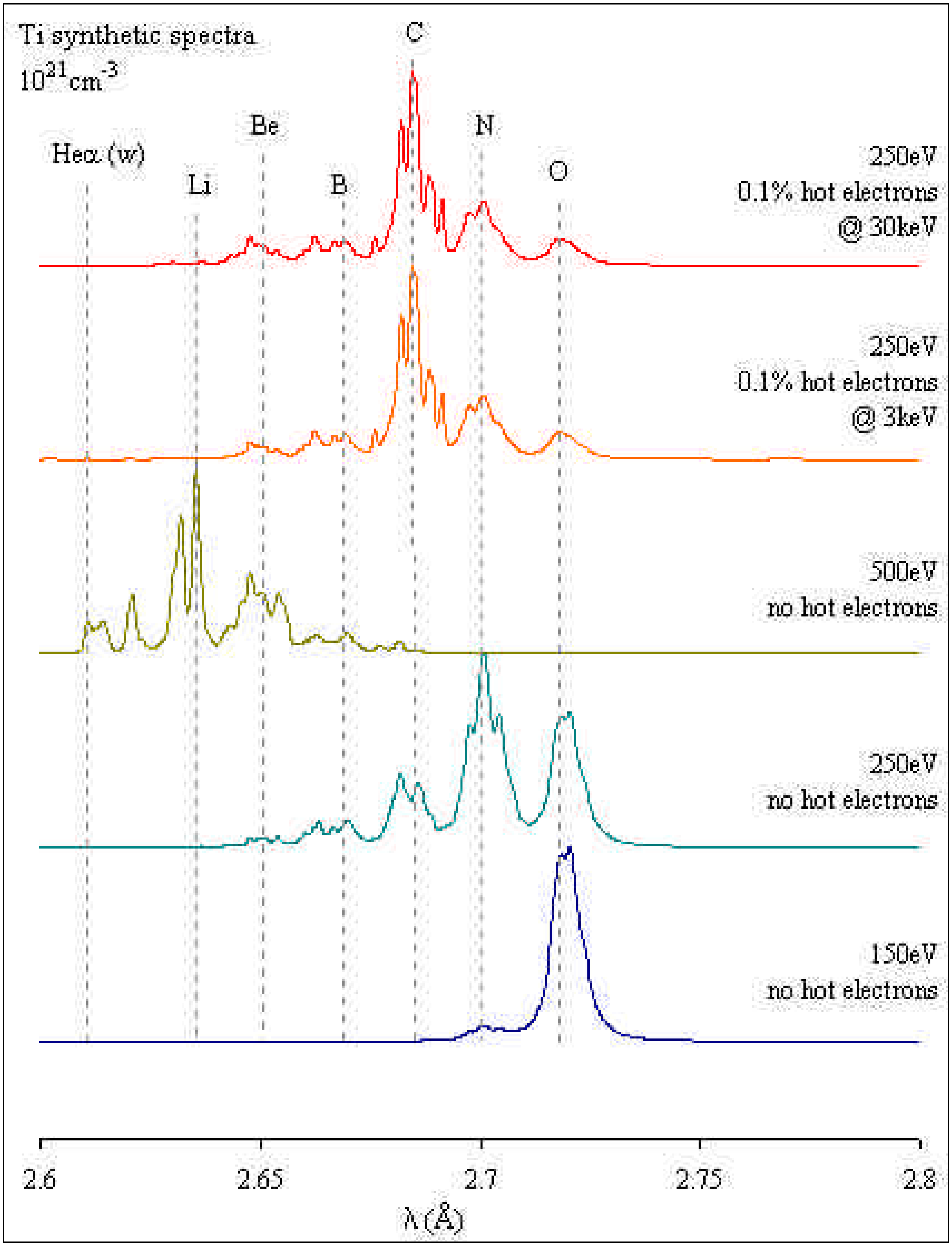

Fig. 8. Effect of Te and hot electrons on the "cooler spectral region" of Ti spectra.

T_e and electron beam fractions were determined for Ti x-pinches. For each experimental spectrum, line shapes were determined. Then, synthetic spectra were constructed with these line shapes over a T_e range of 1-2keV with f from 0-10%. The best fits of He_γ, He_β and satellites, and Ly_α and satellites in all experimental cases indicate the presence of hot electrons in the hot plasma regions. This fitting procedure only determines T_e to ± 100eV and f to a factor of two, since decreasing T_e by 50-100eV and increasing f by 0.5-1% in each case gives fits that are only slightly inferior to the ones chosen. The temperature of the cool region without hot electrons was determined by finding the best fit to the N- and O-like features; T_e of the cool region could be thus determined to within 10eV. The hot electron beam fraction in the cool region was varied until a good fit with the rest of the ionization stage features was found. The hot electron fraction in the cool region was determined to within 0.5%. The Ti x-pinch plasma spectrum was determined to have a hot region with T_e = 1.8keV and f = 4% hot electrons and a cool region with T_e =200eV and f = 6.

In conclusion, the K-shell Ti model developed at the NTF is already useful as a temperature and electron beam fraction diagnostic. Further improvements to increase precision and robustness are necessary and well within sight: efforts to include Ti K_α , opacity and polarization properties of K-shell lines have already begun. The detailed modeling of the polarization-dependent features of Ti is the subject of another publication.

Polarization in X-ray lines of Fe ions is not observed with these LiF crystals; the corresponding Bragg angle is 27^O , and the measured ratio I_{II}/I for the resonance line Heα and an intercombination line y is the same in horizontal and vertical spectra.

II. L-shell x-ray spectropolarimetry

Recently, we have shown that polarization of K-shell line emission can be used to diagnose the presence of particle beams in plasmas, whereas the polarization of L-shell line emission can be used to diagnose the magnetic field in plasmas. L-shell spectra of Ti, Fe, and Mo have been calculated to select the spectral lines most suitable for this diagnostic. The typical L-shell Mo x-pinch spectrum is shown in Fig. 9.

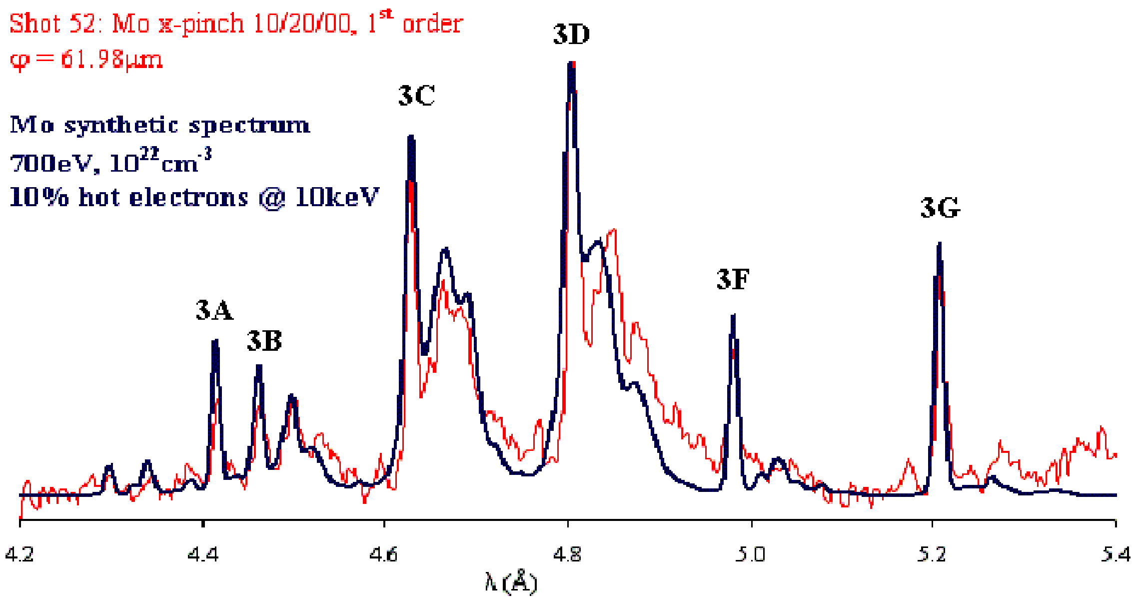

Fig. 9. Comparison of experimental and theoretical spectra of Mo x-pinch plasmas produced on 10/20/2000 (shot 52).

The brightest lines, labeled with letters 3A-3G, belong to Ne-like Mo. The group of lines between 3B and 3C is generated mostly by F-like Mo and the groups between 3C and 3F are mostly Na-like and Mg-like satellite lines. The relative intensities of these features vary from shot to shot and indicate variations of plasma conditions.

Our calculations for Ti are presented in the another publication in this volume (Shlyaptseva at all, ibid). Similar calculations performed for Fe ion lines indicate more L-shell lines suitable for this diagnostic: Ne-like lines 3A (Rα changes from 0 to 0.63), 3B (Rα changes from 0 to 0.95), 3C (Rα changes from 0 to 0.11), and 3D (Rα changes from 0 to 0.73). The vertical line with channels 3 and 4 (Fig. 2) is ready to be used for L-shell spectropolarimetry. We did not succeed yet to produce a good quality L-shell Fe spectrum in a vertical line: one of the reasons is the strong x-ray beam going upwards. Moreover, an analysis of explosions of different types of Fe-pinches has shown that this element has very different pinching properties from Ti and Mo. In particular, we have found that Mo x-pinches produce the brightest L-shell spectra of all elements investigated. It leads us to the conclusion that Mo rather than Fe x-pinches will be used in future diagnostics of the magnetic field. Such experiments are under development.

III. X-ray spectropolarimetry of Ti K-shell emission at LLNL EBIT.

A major thrust of the spectroscopy program at EBIT has been to develop techniques to model, more realistically, the effects of plasma electron energy distributions on the spectra. The goal is to look for electron temperature diagnostics, and signatures of Maxwellian and non-Maxwellian energy distributions. To this end Ti spectra were gathered while the electron beam energy was swept through a carefully synchronized pattern to replicate a Maxwellian. The use of two spectrometers with crystals of differing polarization sensitivities to gather spectra simultaneously allows the determination of the line polarizations. These polarization-sensitive spectra, generated by the Maxwellian electron beam at EBIT, are making a very important contribution to the plasma polarization spectroscopy program at the NTF. In particular, the study of multiply-charged Ti ion spectra will help in the interpretation of the polarization-sensitive experiments using Ti x-pinches at the NTF. The ability of post-experiment processing of event-mode EBIT data allows the separation of the dielectronic satellite lines and structures from the direct excitation lines that are strongly blended in the plasma environment. This provides the opportunity to study separately the polarization properties of spectra produced by different processes, and well-defined electron distribution functions, and to apply the results to the diagnostics of z-pinch plasma experiments.

X-ray line polarization of heliumlike Ti^{20+} excited by a monoenergetic electron beam at LLNL EBIT was measured by Beiersdorfer et al [5]. In the present paper we use the same technique to measure polarization-sensitive Ti spectra but they were generated by a quasi-Maxwellian electron beam and were accumulated simultaneously using two individual von Hamos spectrometer setups. The spectrometers observed photons emitted along axes perpendicular to the electron beam axis, and their dispersion planes were also normal to the electron beam axis. One spectrometer used a Si (220) crystal and the other one a Ge (111) crystal. These crystals were chosen because of appropriate integrated reflectivities R_{II} and R for x-rays polarized perpendicular and parallel respectively to the electron beam axis, which in turn is parallel and perpendicular to the spectrometers dispersion plane in the present experimental setup. In particular, the relative reflectivity, $R=R\ /R_{II}$ indicates the polarization sensitivity of the crystal, as the intensity of the observed lines is given by the relationship $I_{obs}=R_{II} \times I_{II} + R \ \times \ I$, where I_{II} and I are the x-ray intensities for polarization components parallel and perpendicular respectively to the electron beam axis. Using crystals with very different values for R provides the most polarization sensitivity to the experiment. R is strongly dependent on the Bragg angle. The Si (220) and Ge (111) crystals have a spacing corresponding at the wavelengths of interest to nominal Bragg angles of 43^{O} and 23.5^{O}, respectively. Post-experiment processing of event-mode EBIT data produce two different data sets: the first experimental data set includes two spectra recorded simultaneously by two crystals corresponding to the spectral lines produced via electron impact excitation (Fig. 10), and the second experimental data set includes two spectra recorded simultaneously by two crystals corresponding to the satellite lines produced via dielectronic recombination (Fig. 11).

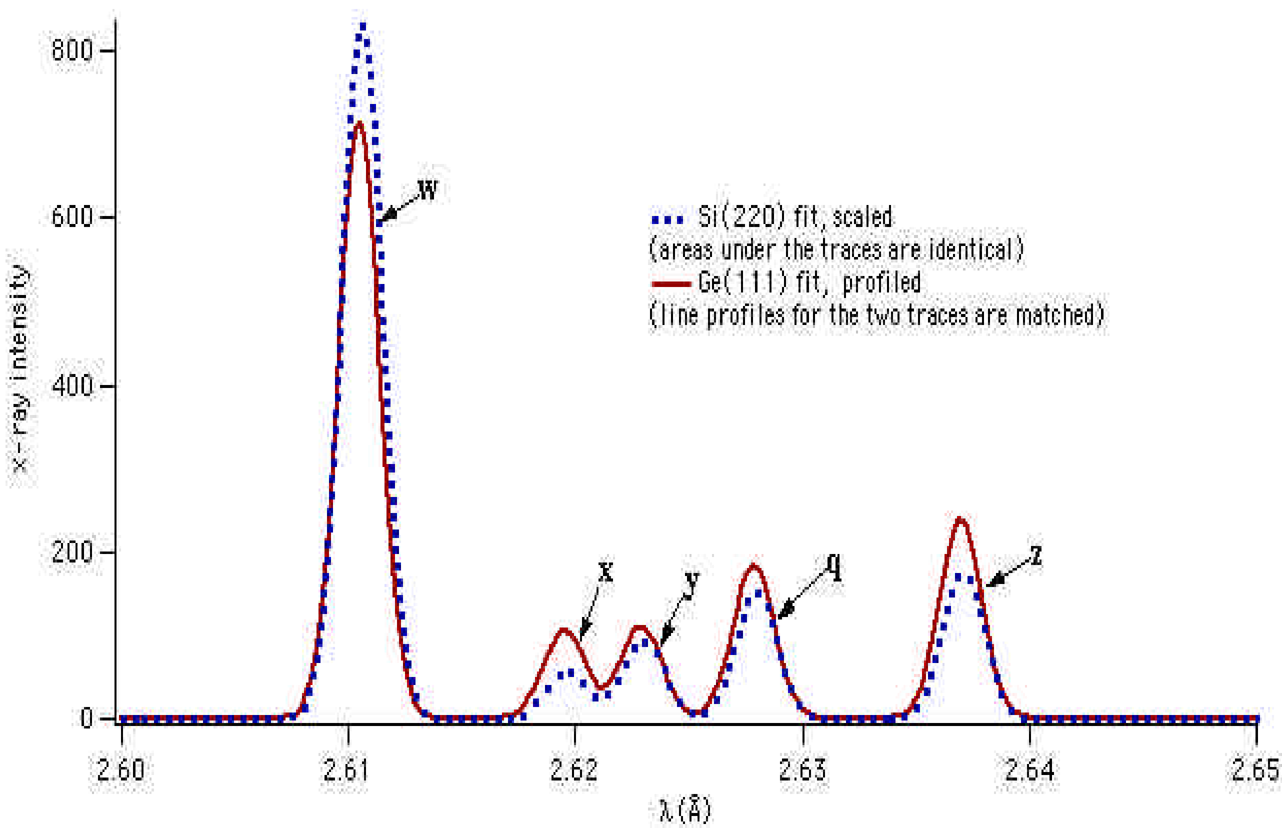

Fig. 10. Experimental direct electron excitation spectra of He-like Ti produced by a quasi-Maxwellian electron beam simultaneously recorded by Si 220 and Ge 111 crystals.

In Fig. 10, the first experimental data set is shown which includes the most prominent He-like resonance line w at λ=2.6105 Å together with other lines excited by electron impact, such as He-like lines z, x, and y and Li-like inner-shell satellites of Ti ions, produced by the unidirectional electron beam with a quasi-Maxwellian distribution function. The comparison of measured relative intensities of the He-like Ti lines w, z, x, and y, and the Li-like Ti line q produced by the quasi-Maxwellian (present paper) and monoenergetic electron beam [5] is presented in Table 3.

Table 3. The comparison of experimental relative intensities of the He-like Ti lines z, x, and y, and Li-like Ti line q to the line w produced by the quasi-Maxwellian and the monoenergetic electron beam at LLNL EBIT.

	Present paper			Ref. [5]		
	Si(220)	Ge(111)		Si(220)	Si(111)	
	I_1	I_2	I_1/I_2	I_3	I_4	I_3/I_4
z/w	0.212	0.335	0.633	0.258	0.343	0.752
x/w	0.068	0.145	0.469	0.102	0.191	0.534
y/w	0.113	0.153	0.739	0.147	0.235	0.625
q/w	0.184	0.255	0.722	0.313	0.316	0.99

The x-ray spectrum of He-like Ti excited by the monoenergetic electron beam was measured at an energy just above the electron-impact excitation threshold (4800 eV) [5]. From the ratio I_3/I_4 for four lines z, x, y, and q it follows that the line q has a maximum, positive polarization almost equal to the line w and the line x has the lowest, negative polarization. In the present paper, the electron beam was set to model a Maxwellian distribution function with T_M=2.3 keV in the energy range from 0.6 keV up to 11.85 keV. To calculate line polarization, the corresponding cross sections of M-sublevels are integrated over 2.5 times threshold. The polarization of the line w undergoes a small change for these electron energies, the calculated value is equal to 58%, which is close to the value calculated for the monoenergetic beam. The lines z and x have the negative values of polarization at the threshold, which monotonically decrease with the energy. The line y has also the negative polarization at the threshold, but the line y is the only one line which polarization undergoes considerable changes from a negative to a positive value in the range from the excitation threshold up to 2.5 times excitation thresholds. The comparison of I_3/I_4 and I_1/I_2 for the z, x, and y lines proves that: the ratio decreases for the lines z and x and they become more negatively polarized, the ratio increases for the line y, which become more positively polarized. The comparison of these ratios for the line q indicates considerable decrease in the value of polarization, which does not agree with theoretical calculations. To complete the study of polarization properties of these lines produced by a quasi-maxwellian electron beam it is necessary to include the higher-n satellites [6,7]. Specifically, we are estimating the contribution of unresolved dielectronic satellites due to transitions $1s^2 3l$-$1s2l'3l''$ into intensities of polarized w, x, y, and q lines. We have already succeed in the interpretation of the polarization-dependent spectra of Li- and Be-like dielectronic satellites due to transitions with n=2. Using the same experimental data set and the same technique, we have resolved polarization-sensitive dielectronic satellite transitions with n=3 separately from direct excitation lines and are working on their analysis. It will provide us the important answer how the unresolved dielectronic satellite structures from higher Rydberg states can affect the polarization of resonance and forbidden lines in plasma.

By analyzing the second experimental data set (Fig. 11), we studied the polarization properties of dielectronic satellites of Li- and Be-like Ti, produced by the unidirectional electron beam with a quasi-Maxwellian distribution function. The details of calculations of atomic and polarization characteristics of Kα transitions in Ti ions are discussed in another publication of the same volume (Shlyaptseva at al, ibid.). The comparison of theory and the experimental data shows encouraging agreement.

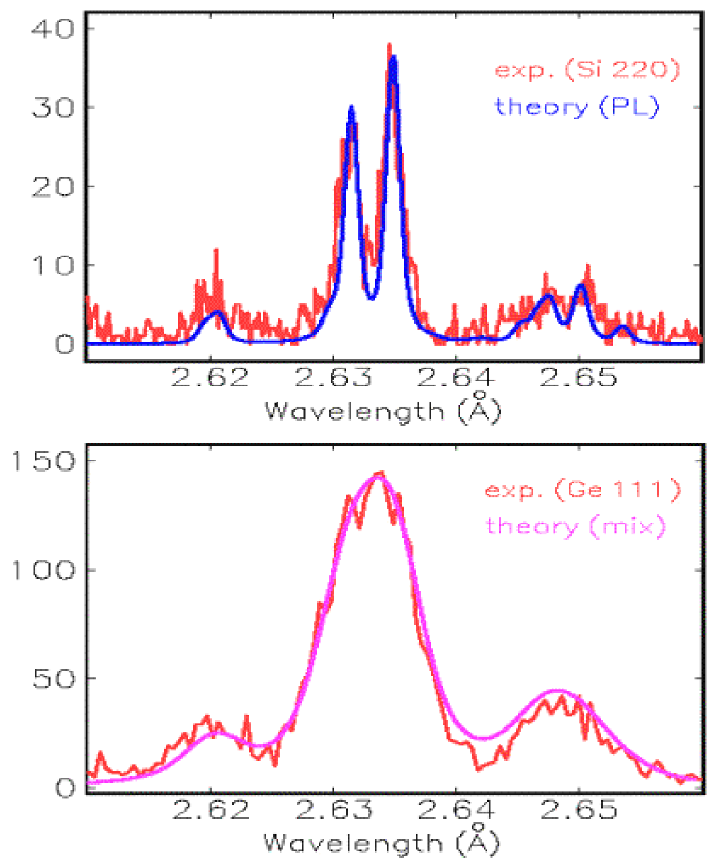

Fig. 11. Comparison of experimental and theoretical dielectronic recombination spectra of He-like Ti produced by a quasi-Maxwellian electron beam simultaneously recorded by Si 220 and Ge 111 crystals.

ACKNOWLEDGMENT

Work was performed by the University of California Lawrence Livermore National Laboratory was performed under the auspices of the Department of Energy under contract W-7405-ENG-48.

REFERENCES

1. A.S. Shlyaptseva, S. B. Hansen, V.L. Kantsyrev, B.S. Bauer, D.A. Fedin, N. Ouart, S.A. Kazantsev, A.G. Petrashen, U.I. Safronova, "X-ray spectropolarimetry of high-temperature plasmas", Rev. Sci. Instrum., 72, 1(II), pp. 1241-1244, 2001.

2. V. Kantsyrev, B. Bauer, A. Shlyaptseva, D. Fedin, S. Hansen, R. Presura, S. Batie, A. Oxner, B. LeGalloudec, H. Faretto, D. Chamberlain, N. Ouart, A. Jones, H. LeBeau, M. Gharaibeh, "Advanced x-ray and EUV diagnostics and first application to x-pinch plasma experiments at the Nevada Terawatt Facility", Rev. Sci. Instrum., v.72, 1(II), pp.663-667, 2001.

3. V.L. Kantsyrev, A.S. Shlyaptseva, B.S. Bauer, D.A. Fedin, R. Presura, S. Fuelling, S. Hansen, S. Batie, A. Oxner, H. Faretto, N. Ouart, S. Keely, H. LeBeau, D. Chamberlain, "X-ray temporal, spatial and spectral study of 0.9 MA x-pinch Ti, Fe, Mo, W and Pt radiation sources. Energetic electron beam and hard x-ray generation", PPPS-2001 Conf. Proc. Book, 2001 (in press)

4. V.L. Kantsyrev, B.S. Bauer, A.S. Shlyaptseva, D.A. Fedin, S. Hansen, R.Presura, S. Fuelling, S. Batie, A. Oxner, H. Faretto, N. Ouart, S. Keely, H. LeBeau, D. Chamberlain. "Powerful microfocus x-ray and hard x-ray 1 MA x-pinch plasma source for imaging, spectroscopy, backlighting, and polarimetry". Proc.SPIE , v. 4502, 2001 (in press).

5. P. Beiersdorfer, G. Brown, S. Utter, P. Neill, K.J. Reed, A.J. Smith, and R.S. Thoe, "Polarization of K-shell transitions of Ti^{19+} and Ti^{20+} excited by an electron beam", Phys. Rev. A, v. 60, 5, pp. 4156-4159, 1999.

6. S. Chantrenne, P. Beiersdorfer, R. Cauble, and M.B. Schneider, "Measurement of Electron Impact Excitation Cross Sections for Heliumlike Titanium", Phys. Rev. Let., v. 69, 2, pp. 265-268, 1992.

7. M. Bitter, K.W. Hill, M. Zarnstorff, S. von Goeler, R. Hulse, L.C. Johnson, N.R. Sauthoff, S. Sesnic, and K.M. Young et al., "Satellite spectra for heliumlike titanium. II.", Phys. Rev. A, v. 32, 5, pp. 3011-3029, 1985.

University of California
Lawrence Livermore National Laboratory
Technical Information Department
Livermore, CA 94551